Vol 17 No 12, December 2008
1674-1056/2008/17(12)/4627-08

Chinese Physics B

© 2008 Chin. Phys. Soc.
and IOP Publishing Ltd

Phase coherence of the electron and hole in a ferromagnetic film in proximity with a superconductor*

Yu Hua-Ling(郁华玲)†, Wang Zhi-Guo(王之国), and Peng Ju(彭 菊)

Department of Physics, Huaiyin Teachers College, Huaian 223001, *China*

(Received 25 October 2007; revised manuscript received 6 July 2008)

The scattering matrix approach between the clean and dirty limits is developed for the study of tunnelling spectra in a ferromagnetic film in proximity to a superconductor. The minigap and the damped oscillation from '0' to 'π' state in tunnelling conductance are attributed to the phase coherence of the electrons and the corresponding Andreev-reflected holes in the ferromagnetic film. The calculated results provide a reasonable explanation for the behaviour observed in recent experiments.

Keywords: proximity effect, coherent transport, sequential transport
PACC: 7210, 7450

1. Introduction

The superconducting proximity effect is the occurrence of superconducting-like properties in nonsuperconducting materials placed in electric contact with a superconductor. The special reflection process known as Andreev reflection (AR)[1] plays an important role in the superconducting proximity effect. In this process an electron with an energy lower than the superconducting gap in the nonsuperconducting material is reflected back as a hole along with the time-reversed path with the simultaneous generation of a Cooper pair[2] in the superconductor. The electron and the hole having opposite spins and different Fermi momenta are correlated via AR, thus providing an extension of superconductivity into a nonsuperconducting region. In the normal metal/superconductor (NM/S) junctions these correlations decay with the distance from the interface due to a dephasing between the wavefunctions of electrons and holes, thus there appears a proximity-effect-induced superconducting order parameter $F(x)$ in normal metal, and it decays with increasing distance from the interface. If the nonsuperconductor is a ferromagnet, the electrons and holes are under the exchange field of the ferromagnet, which results in the energy shift between these quasiparticles and the creation of a finite centre-of-mass momentum $Q = 2h_0/\hbar v_{\rm F}$ of Cooper pairs, where $2h_0$ is the exchange energy corresponding to the difference in energy between spin-up and spin-down bands in ferromagnet and $v_{\rm F}$ is the Fermi velocity. In this case, $F(x)$ exhibits damped oscillations[2−4] with increasing distance from the interface. These oscillations were originally investigated by Fulde and Ferrell[5] and Larkin and Ovchinnikov.[6] The state with positive $F(x)$ is usually called the '0' state and that with negative $F(x)$ called the 'π' state. A transition from '0' to 'π' state has been already reported by many authors. Kontos *et al*[7] studied differential conductance spectra in $Al/Al_2O_3/PdNi/Nb$ tunnel junctions where PdNi is a thin ferromagnetic film and Nb is an s-wave superconductor. The observed density of states (DOS) in ferromagnet shows the '0' or 'π' state shape when the thickness of the ferromagnetic layer is, respectively, smaller or larger than $\xi_{\rm F}$, where $\xi_{\rm F} = \hbar v_{\rm F}/2h_0$ is the coherence length in ferromagnet. Many works[8−19] have shown that inhomogeneous superconductivity can be induced in ferromagnet by the proximity effect in ferromagnet/superconductor (F/S) structures and that the DOS for the '0' and 'π' states observed in Ref.[7] can be reproduced by their theoretical calculations. However, how the magnitude of h_0 affects DOS and whether it can lead to the transition from '0' state to 'π' state when the thickness of

*Project supported by the Natural Science Foundation of Education Bureau of Jiangsu Province, China (Grant No 07KJD140024), and Jiangsu key Laboratory for Chemistry of Low-Dimensional Materials (Huaiyin Teachers College), China.
†E-mail: hlyu7505@yahoo.com.cn

ferromagnet is fixed have not been discussed. This is one of the motivations in this work.

Recently, the minigap in the local density of states (LDOS) in nonsuperconductor induced by the superconducting proximity effects has attracted much attention in experimental and theoretical investigations.[20−25] A fully opened minigap was found by Moussy, Courtois and Pannetier[24] in a very thin ($L = 20\,\mathrm{nm}$) Au layer on top of a Nb dot with the help of a very low temperature (60 mK) scanning tunnel microscopy (STM). It is well worth to mention that Gupta *et al*[26] also observed an ideal minigap in an Au–Nb bilayer with the smallest Au thickness ($L = 10\,\mathrm{nm}$) under the same experimental conditions. They found that a nonzero LDOS near E_F appears at $L = 30\,\mathrm{nm}$ and gradually increases with L. In addition, an anomalous minigap width evolution was observed. As pointed out by Gupta *et al*,[26] these new features found in the cleaner samples cannot be explained within the quasiclassical theory which was well established in the dirty limit. As a result, a theoretical approach in the clean limit or in the intermediate case is necessary for addressing this issue. Very recently, Kontos *et al*[27] studied differential conductance spectra in $\mathrm{Al/Al_2O_3/NM/Nb}$ tunnel junctions with the thickness of NM fixed (5 nm), where NM is a paramagnetic metallic film, such as Ag, Pt, Pd or $\mathrm{Pd_{1-}}_x\mathrm{Ni}_x$ ($x \leq 0.024$). The observed normalized conductance also exhibits a subgap with nonzero LDOS around E_F, and the subgap width decreases with increasing susceptibility of NM. Although the Usadel equations were used to fit the experimental data, since there is a crossover from a clean metal to dirty ones, it is highly desirable to develop a theory in the clean limit but including impurity scattering.

In the NM/I/F/I/S (I = insulator, F = ferromagnet, and S = superconductor) structure under consideration, the thin ferromagnet film between two junctions is a typical mesoscopic conductor and NM is an electrode for measurements. In the presence of scattering processes in the ferromagnet layer, a fraction of electrons (holes) transmit coherently while the remainder gets scattered inside the ferromagnet and effectively leaks out of the coherent stream. The transport lies in an intermediate regime between the clean and dirty limits, so that both coherent and sequential processes need to be taken into account. In this work we extend the scattering matrix approach suitable for metallic double tunnel junctions[28] to the NM/I/F/I/S structures by including the coherent and sequential components of the tunnelling conductance. In consideration of electron-like and hole-like quasiparticles (ELQ and HLQ) in the superconductor and the spin degree of freedom in the ferromagnet, the original 2×2 S-matrices should be extended to 8×8 ones. If the spin–flip scattering is neglected, however, the 8×8 S-matrix may be decoupled into two sets of 4×4 matrices for the spin-σ ELQ and spin-$\bar{\sigma}$ HLQ. The tunnelling conductance of the NM/I/F/I/S structures is obtained as a function of thickness L of the middle ferromagnet film. Its expression is given by reflection and transmission coefficients of two independent junctions. These coefficients in the F/I/S junction can be obtained using the Bogoliubov–de Gennes (BdG) equation[29] and the theoretical approach developed by Blonder *et al*.[30] Our calculations show that the complete coherent transport leads to a fully opened minigap in the LDOS while the sequential component makes the LDOS peaks lower and the LDOS within the minigap rise up. For the case of $h_0 = 0$ in the ferromagnet film, with increasing L, the distance between two peaks of the minigap decreases and the amplitude of gap-like structures decays, accompanied by a dephasing between the wavefunctions of electrons and holes. For the case of $h_0 \neq 0$, the LDOS displays a damped oscillation with the thickness of ferromagnet or exchange energy h_0, exhibiting a transition from '0' to 'π' state. We conclude that the exchange energy can induce the transition from '0' to 'π' state. The presence of scattering which breaks up the phase coherence provides an explanation for the nonzero LDOS within the minigap observed widely in experiments except that the ferromagnet film is thin enough. Our calculated results may reproduce main features of the abnormal minigap in the LDOS observed in the experiments.[26,27]

2. Model and theory

We first consider the coherent transport of quasiparticles in the middle ferromagnet region for current flow through an NM/I/F/I/S double-barrier structure. For such a structure, if the middle ferromagnet region between two tunnel barriers is a few nanometres in length, the coherent transport plays a dominant role. We extend the scattering matrix approach used in the NM/I/NM/I/NM structure[28] to the present double-junction including the ferromagnet and superconductor. Since the superconductor has two types of

quasiparticles (ELQ and HLQ) and the ferromagnet has the spin degree of freedom, the 2×2 S-matrix should be extended to an 8×8 matrix. If the spin-flip scattering is neglected, the spin-dependent 8×8 S-matrix may be decoupled to the 4×4 S-matrix. Let us first consider the right F/S junction in Fig.1, in which a_2 and b'_3 (d_2 and c'_3) indicate the incoming wave amplitudes for the ELQ (HLQ) from both sides,

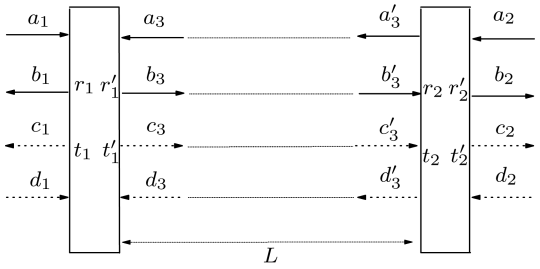


Fig.1. Schematic diagram of NM/I/F/S junction in which two potential barriers are placed in series with a coherent distance L. The problem is to find the scattering S-matrix of the composite structure.

and b_2 and a'_3 (c_2 and d'_3) indicate the outgoing wave amplitudes for the ELQ (HLQ). They satisfy the following relation: via a 4×4 S-matrix.

$$\begin{pmatrix} a'_3 \\ d'_3 \\ b_2 \\ c_2 \end{pmatrix} = \begin{pmatrix} r_{\rm ee2} & r_{\rm he2} & t'_{\rm ee2} & t'_{\rm he2} \\ r_{\rm eh2} & r_{\rm hh2} & t'_{\rm eh2} & t'_{\rm hh2} \\ t_{\rm ee2} & t_{\rm he2} & r'_{\rm ee2} & r'_{\rm he2} \\ t_{\rm eh2} & t_{\rm hh2} & r'_{\rm eh2} & r'_{\rm hh2} \end{pmatrix} \begin{pmatrix} b'_3 \\ c'_3 \\ a_2 \\ d_2 \end{pmatrix}. \quad (1)$$

Here the subscript 2 of the matric elements stands for the right (second) junction. For an ELQ incident on the interface from left (right), $r_{\rm ee2}$ ($r'_{\rm ee2}$) is the normal-reflection amplitude and $r_{\rm eh2}$ ($r'_{\rm eh2}$) is the AR amplitude; $t_{\rm ee2}$ ($t'_{\rm ee2}$) is the amplitude of transmission within the same branch and $t_{\rm eh2}$ ($t'_{\rm eh2}$) is that between the ELQ and HLQ branches. For an HLQ incident on the interface from the left (right), $r_{\rm hh2}$ ($r'_{\rm hh2}$), $r_{\rm he2}$ ($r'_{\rm he2}$), $t_{\rm hh2}$ ($t'_{\rm hh2}$), and $t_{\rm he2}$ ($t'_{\rm he2}$) have the similar definitions. All the S-matrix elements in Eq.(1) can be obtained in an F/S single junction by using the BTK approach,[30] whose expressions will be given in the Appendix. We then consider the left NM/I/F tunnel junction of Fig.1. Similarly, we have

$$\begin{pmatrix} b_1 \\ c_1 \\ b_3 \\ c_3 \end{pmatrix} = \begin{pmatrix} r_{\rm ee1} & 0 & t'_{\rm ee1} & 0 \\ 0 & r_{\rm hh1} & 0 & t'_{\rm hh1} \\ t_{\rm ee1} & 0 & r'_{\rm ee1} & 0 \\ 0 & t_{\rm hh1} & 0 & r'_{\rm hh1} \end{pmatrix} \begin{pmatrix} a_1 \\ d_1 \\ a_3 \\ d_3 \end{pmatrix}. \quad (2)$$

Here subscript 1 of the matric elements stands for the right (first) junction, and all the AR coefficients and transmission amplitudes between the ELQ and HLQ branches vanish due to the absence of the superconductor. All the S-matrix elements in Eq.(2) are obtained in an NM/I/F single tunnel junction, their expressions being also given in the Appendix. If the quasiparticle transport is coherent, the wavevector of the quasiparticle remains unchanged, so that a_3 (b_3, c_3, d_3) is related to a'_3 (b'_3, c'_3, d'_3) by a phase difference, i.e.,

$$\begin{aligned} a'_3 &= a_3 {\rm e}^{-{\rm i}k_{\rm e}^{\sigma}L},\ b'_3 = b_3 {\rm e}^{{\rm i}k_{\rm e}^{\sigma}L}, \\ c'_3 &= c_3 {\rm e}^{-{\rm i}k_{\rm h}^{\bar\sigma}L},\ d'_3 = d_3 {\rm e}^{{\rm i}k_{\rm h}^{\bar\sigma}L}, \end{aligned} \quad (3)$$

where $k_{\rm e}^{\sigma}$ is the perpendicular component of Fermi wave vector for spin-σ electrons in ferromagnet and $k_{\rm h}^{\bar\sigma}$ for spin-$\bar\sigma$ holes. It is straightforward to eliminate a_3, a'_3, b_3, b'_3, c_3, c'_3, d_3 and d'_3 from Eqs.(1)–(3) to obtain

$$\begin{pmatrix} b_1 \\ c_1 \\ b_2 \\ c_2 \end{pmatrix} = \begin{pmatrix} r_{\rm ee} & r_{\rm he} & t'_{\rm ee} & t'_{\rm he} \\ r_{\rm eh} & r_{\rm hh} & t'_{\rm eh} & t'_{\rm hh} \\ t_{\rm ee} & t_{\rm he} & r'_{\rm ee} & r'_{\rm he} \\ t_{\rm eh} & t_{\rm hh} & r'_{\rm eh} & r'_{\rm hh} \end{pmatrix} \begin{pmatrix} a_1 \\ d_1 \\ a_2 \\ d_2 \end{pmatrix}. \quad (4)$$

The normal reflection and AR probabilities for the coherent tunnelling can be obtained as

$$\begin{aligned} R_{\rm ee}^{\rm c} &= |r_{\rm ee}|^2 \\ &= \left| \frac{(t_{\rm ee1}^2 - r_{\rm ee1}r'_{\rm ee1})[r'_{\rm hh1}r_{\rm eh2}^2 - (r_{\rm hh2}r'_{\rm hh1} - {\rm e}^{2{\rm i}k_{\rm h}^{\bar\sigma}L})r_{\rm ee2}] - (r_{\rm hh2}r'_{\rm hh1} - {\rm e}^{2{\rm i}k_{\rm h}^{\bar\sigma}L})r_{\rm ee1}{\rm e}^{-2{\rm i}k_{\rm e}^{\sigma}L}}{(r_{\rm hh2}r'_{\rm hh1} - {\rm e}^{2{\rm i}k_{\rm h}^{\bar\sigma}L})(r'_{\rm ee1}r_{\rm ee2} - {\rm e}^{-2{\rm i}k_{\rm e}^{\sigma}L}) - r'_{\rm ee1}r'_{\rm hh1}r_{\rm eh2}^2} \right|^2, \end{aligned} \quad (5)$$

$$R_{\rm eh}^{\rm c} = |r_{\rm eh}|^2 = \left| \frac{t_{\rm ee1}r_{\rm eh2}t'_{\rm hh1}}{(r_{\rm hh2}r'_{\rm hh1} - {\rm e}^{2{\rm i}k_{\rm h}^{\bar\sigma}L})(r'_{\rm ee1}r_{\rm ee2} - {\rm e}^{-2{\rm i}k_{\rm e}^{\sigma}L}) - r'_{\rm ee1}r'_{\rm hh1}r_{\rm eh2}^2} \right|^2. \quad (6)$$

Next, we consider the sequential tunnelling case in which the quasiparticle in the middle ferromagnet undergoes scattering. In this case, we can obtain $R_{\rm ee}^{\rm s}$ and $R_{\rm eh}^{\rm s}$ by summing up the probabilities for the direct normal

reflection at the left NM/I/F interface, and for the normal reflection and AR with one reflection at the right F/S interface, with two reflections, three reflections and so on.[28] Since there may be either normal reflection or AR at the F/S interface, the situation is relatively more complicated. Taking into account all the possible reflection processes and after lengthy algebraic calculation, we obtain

$$R^{\rm s}_{\rm ee} = \frac{(T^2_{\rm ee1} - R_{\rm ee1}R'_{\rm ee1})[R'_{\rm hh1}R^2_{\rm eh2} - (R_{\rm hh2}R'_{\rm hh1} - 1)R_{\rm ee2}] - (R_{\rm hh2}R'_{\rm hh1} - 1)R_{\rm ee1}}{(R_{\rm hh2}R'_{\rm hh1} - 1)(R'_{\rm ee1}R_{\rm ee2} - 1) - R'_{\rm ee1}R'_{\rm hh1}R^2_{\rm eh2}}, \tag{7}$$

$$R^{\rm s}_{\rm eh} = \frac{T_{\rm ee1}R_{\rm eh2}T'_{\rm hh1}}{(R_{\rm hh2}R'_{\rm hh1} - 1)(R'_{\rm ee1}R_{\rm ee2} - 1) - R'_{\rm ee1}R'_{\rm hh1}R^2_{\rm eh2}}, \tag{8}$$

where $T_{\rm ee1} = |t_{\rm ee1}|^2$, and the others in Eqs.(7) and (8) can be obtained in the same way. Alternatively, $R^{\rm s}_{\rm ee}$ and $R^{\rm s}_{\rm eh}$ given above can be obtained by remaking Eqs.(1), (2) and (4). Each component of the column matrices is redefined as either an incoming or outgoing quasiparticle flow, and the S-matrix element $s(m,n)$ is replaced by either reflection or transmission probabilities $|s(m,n)|^2$. From the current continuity conditions in the middle ferromagnet layer for each spin channel: $a'_3 = a_3$, $b'_3 = b_3$, $c'_3 = c_3$ and $d'_3 = d_3$, Eqs.(7) and (8) can be confirmed.

In the following, we consider a combination of the coherent tunnelling with the sequential one. For a fraction of the quasiparticle flow due to sequential transport, a quasiparticle first tunnels into the middle ferromagnet and then, after losing memory of its phase, tunnels out of the ferromagnet. We introduce the phase-coherence length l_ϕ in the ferromagnet and replace $k^\sigma_{\rm e}$ ($k^{\bar\sigma}_{\rm h}$) in the exponents by $k^\sigma_{\rm e} + {\rm i}/l_\phi$ ($k^{\bar\sigma}_{\rm h} - {\rm i}/l_\phi$), where $1/l_\phi$ is much smaller than the Fermi wave vector $k^\sigma_{\rm e}$ or $k^{\bar\sigma}_{\rm h}$. For the fully coherent transport ($l_\phi \to \infty$), we have $R^{\rm c}_{\rm ee} + R^{\rm c}_{\rm eh} + T^{\rm c}_{\rm ee} + T^{\rm c}_{\rm eh} = 1$. For finite l_ϕ, we define $\alpha = 1 - R^{\rm c}_{\rm ee} - R^{\rm c}_{\rm eh} - T^{\rm c}_{\rm ee} - T^{\rm c}_{\rm eh}$ as the weight per cent of the sequential transport, α should be a function of both L and h_0, and $\alpha = 0$ for $L \ll l_\phi$ and $\alpha = 1$ for $L \gg l_\phi$. Using α to replace $T_{\rm ee1}$ in Eqs.(7) and (8), we obtain the total probabilities of the normal reflection and AR

$$R_{\rm ee} = R^{\rm c}_{\rm ee} + \frac{\alpha[R'_{\rm hh1}R^2_{\rm eh2} - (R'_{\rm hh1}R_{\rm hh2} - 1)R_{\rm ee2}]T'_{\rm ee1}}{(R_{\rm hh2}R'_{\rm hh1} - 1)(R'_{\rm ee1}R_{\rm ee2} - 1) - R'_{\rm ee1}R'_{\rm hh1}R^2_{\rm eh2}}, \tag{9}$$

$$R_{\rm eh} = R^{\rm c}_{\rm eh} + \frac{\alpha R_{\rm eh2}T'_{\rm hh1}}{(R_{\rm hh2}R'_{\rm hh1} - 1)(R'_{\rm ee1}R_{\rm ee2} - 1) - R'_{\rm ee1}R'_{\rm hh1}R^2_{\rm eh2}}, \tag{10}$$

where the coherent components $R^{\rm c}_{\rm ee}$ and $R^{\rm c}_{\rm eh}$ have been given in Eqs.(5) and (6). Finally, the tunnelling conductance is given by

$$G = \sum_{\sigma=\uparrow,\downarrow} \frac{2e^2}{h}(1 - R_{\rm ee} + R_{\rm eh}). \tag{11}$$

3. Results and discussions

We have studied first the tunnelling conductance of the NM/I_1/NM/S double junctions by letting $h_0 = 0$ in NM/I_1/F/S junctions, in which the NM/S interface is in ohmic contact. The parameters used in the calculations are taken as follows. The dimensionless potential strength of barrier I_1 is $Z_1 = 4.0$, $Z_2 = 0$ for the NM/S ohmic contact, the Fermi energy $E_{\rm F} = 1.4\,{\rm eV}$, and the superconducting energy gap $\Delta_0 = 1.4\,{\rm meV}$, $l_\phi = 4\xi_{\rm S}$ with $\xi_{\rm S} = \hbar v_{\rm F}/2\Delta_0$ the coherent length in superconductor. Figure 2 shows the energy dependence of conductances for different thickness L. The conductance is normalized by its value at $E = 3\Delta_0$, beyond which the conductance is almost constant. They exhibit BCS-like minigap behaviour. For the smallest thickness ($L = 0.1\xi_{\rm S}$), the sequential component has only a small effect, and the normalized conductance exhibits two peaks at $E = \pm\Delta_0$ and a gap nearly appears at $|E| < \Delta_0$, which is very close to that in the bulk superconductor. With increasing L, the sequential component plays an important role. The normalized conductances within the minigap increase, which are strikingly different from zero even for $E = 0$. At the same time, the distance between

the two peaks becomes small and the peak height decreases. It is interesting to note that there are two small dips at $E = \pm\Delta_0$, which actually imply that a larger thickness of NM cannot influence significantly the superconducting gap in the bulk superconductor. These calculated results are consistent with those in Ref.[26].

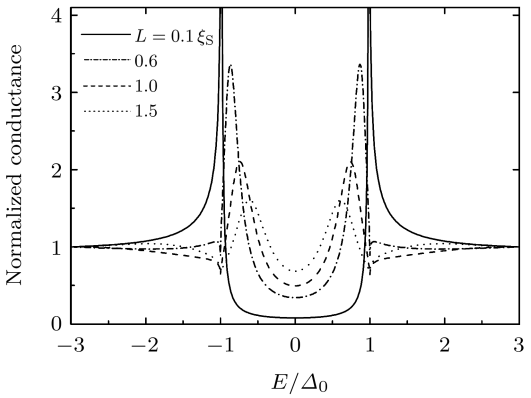


Fig.2. Normalized conductance with $h_0 = 0$ as a function of energy for different thickness L.

Next, we consider the NM/I_1/F/S junctions. Figure 3(a) shows the normalized conductance as a function of the thickness of ferromagnet at $E = 0$ (solid line) and $E = 1.1\Delta_0$ (dotted line) with $h_0/E_F = 0.01$ and $l_\phi = 4\xi_F$, and the other parameters are the same as in Fig.2. Owing to the superconducting proximity effect, a few Cooper pairs are injected into ferromagnet from superconductor and these Cooper pairs can survive for a time corresponding to a travelling length on the order of ξ_F. Together with the interference between the electron (hole) and the AR hole (electron) in the ferromagnet. The normalized conductance displays a damped oscillation with a period of $L = \pi\xi_F$. When the thickness L is smaller than ξ_F, the normalized conductance at $E = 0$ is smaller than the value at $E = 1.1\Delta_0$, which corresponds to the '0' state. When L is larger than ξ_F, the case is reversed and it corresponds to 'π' state. Further increasing L, the sequential component increases gradually and the normalized conductance exhibits a damped oscillation and finally it becomes equal to unity with a dephasing between the wavefunctions of electrons and holes. These calculated results are well consistent with many experimental and theoretical works. Now, we plot the normalized conductance as a function of the exchange energy h_0 for $L = 5\,\text{nm}$ in Fig.3(b). The coherent

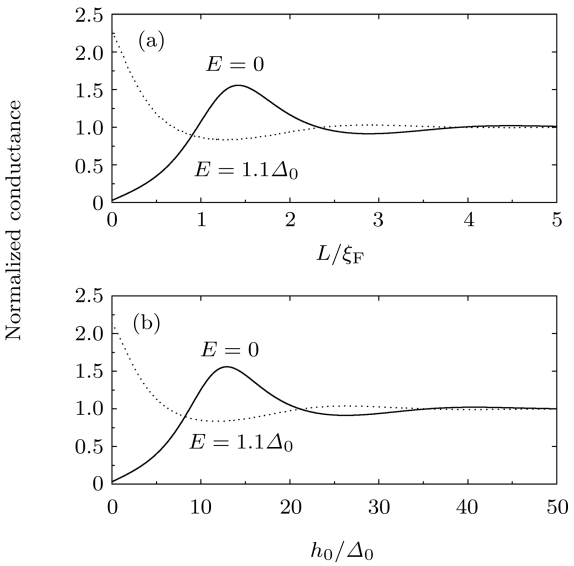


Fig.3. Normalized conductance as a function of (a) thickness of the ferromagnet layer with $h_0 = 10\Delta_0$, (b) exchange energy in ferromagnet with $L = 5\,\text{nm}$, where solid lines stand for $E = 0$ and dotted lines for $E = 1.1\Delta_0$.

length $\xi_F \approx 5\,\text{nm}$ for the exchange energy $h_0 = 9\Delta_0$, so $L < \xi_F$ for $h_0 < 9\Delta_0$ and $L > \xi_F$ for $h_0 > 9\Delta_0$. The normalized conductance also displays a damped oscillation from '0' state to 'π' state with increasing exchange energy h_0, and the period is $h_0 = \pi(9\Delta_0)$, as shown clearly in Fig.4. We plot the energy dependence of normalized conductance for different exchange energy h_0 in Fig.4. The normalized conductance for $h_0 = 0$ is shown in Fig.4(a). There are two peaks at the energy gap edges $E = \pm\Delta_0$ and nearly appears a gap between two peaks, which is similar to that in the bulk superconductor, corresponding to '0' state. In Figs.4(b)–4(j), the exchange energies h_0 equal $3\Delta_0$, $4\Delta_0$, $5\Delta_0$, $10\Delta_0$, $13\Delta_0$, $15\Delta_0$, $18\Delta_0$, $20\Delta_0$, and $28\Delta_0$, respectively. At first, the peaks move gradually towards the centre ($E = 0$) with increasing exchange energy h_0 and there are two dips at $E = \pm\Delta_0$. As shown in Figs.4(b), 4(c) and 4(d), peaks occur at $E = \pm 0.8\Delta_0$ for $h_0 = 3\Delta_0$, $E = \pm 0.7\Delta_0$ for $h_0 = 4\Delta_0$ and $E = \pm 0.6\Delta_0$ for $h_0 = 5\Delta_0$. At the same time, the conductance between the two peaks increases and the amplitude of them decreases. These calculated results are in agreement with the experimental results in Ref.[27]. For $h_0 = 10\Delta_0$, as shown in Fig.4(e), the two peaks arrive at zero energy ($E = 0$), exhibiting two dips at the energy gap edges ($E = \pm\Delta_0$) and a maximum at zero energy ($E = 0$), which corresponds

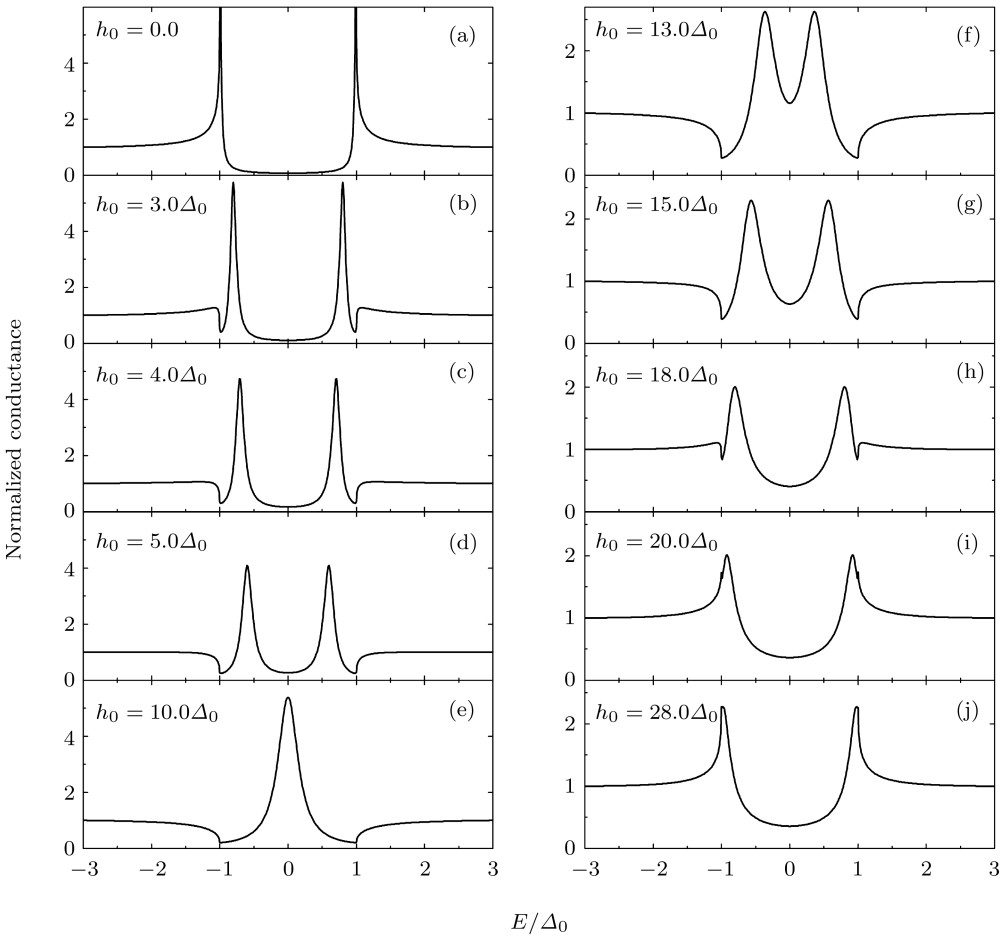


Fig.4. Energy dependence of normalized conductance for different exchange energies. It is gradually reversed from '0" to 'π" state and then from 'π" to '0' state with increasing h_0.

to 'π' state. Further increasing the exchange energy h_0, the dips at $E = \pm\Delta_0$ increase and the maximum at zero energy splits into two peaks, as shown in Figs.4(f) for $h_0 = 13\Delta_0$, and then, the two peaks move gradually away from the centre and the conductance between the two peaks decreases, as shown in Figs.4(g), 4(h) and 4(i), the exchange energies equal $15\Delta_0$, $18\Delta_0$ and $20\Delta_0$ respectively. The case of $h_0 = 28\Delta_0$ is shown in Fig.4(j). There are two peaks at $E = \pm\Delta_0$ and the minimum at $E = 0$, which is similar to Fig.4(a), corresponding to '0' state, but its variation amplitude is very small compared with that in Fig.4(a). Finally, we compare our results with the experimental data in Ref.[27]. As shown in Fig.2 in Ref.[27], the normalized conductance for Ni concentration of 2.4% exhibits two dips at the energy gap edges and the two peaks are situated near $E = \pm 0.6\Delta_0$. This is somewhat like our Fig.4(d). The figure for Ni concentration of 5.5% is the same as our Fig.4(j). There are no experimental line between Ni concentration of 2.4% and 5.5%.

4. Conclusion

The 2×2 scattering matrices for double junctions are extended to the 4×4 ones for the case of superconductor and ferromagnet. In the NM/I_1/NM/S double junctions, due to the superconducting proximity effects, the energy dependence of the normalized conductance exhibits a minigap and its width decreases with increasing L, while the nonzero normalized conductance near the Fermi level increases. These features are in agreement with the experimental results in Ref.[26]. For the NM/I_1/F/S double junctions, the normalized conductance displays a damped oscillation from '0' to 'π' state with not only the thickness of ferromagnet layer but also the exchange energy. We have given the detailed process of the transitions from '0' to 'π' state with increasing exchange energy for a fixed thickness of ferromagnet layer, and we have compared our calculated results with the experimental data in Ref.[27] and wish that the transition from '0' to 'π' state induced by the exchange energy can be observed

in future experiments.

Acknowledgments

We are especially grateful to Professor D. Y. Xing for pointing out the problem in the original manuscript.

Appendix: Expressions for the S-matrix elements in Eqs.(1) and (2)

Consider a planar semi-infinite geometry of Fig.5(a) with a superconductor to the right of $x = 0$ and a ferromagnet to the left. The F/S interface at $x = 0$ is described by a δ-type barrier potential $V_2(x) = Z_2\hbar v_{\rm F}$ where Z_2 is the dimensionless barrier strength. The effective single-particle Hamiltonian is used to describe electrons (holes) in ferromagnet, while superconductor is assumed to be s-wave pairing and described by a BCS-like Hamiltonian. There are four types of quasiparticle injection processes at the F/S interface: electron and hole injection from ferromagnet to superconductor, and ELQ and HLQ injection from superconductor to ferromagnet, as shown in Fig.5(b). As an example, for a spin-σ electron incident on the interface at $x = 0$ from ferromagnet, there are four possible trajectories: normal reflection ($r_{\rm ee2}$), Andreev reflection ($r_{\rm eh2}$), transmission to the superconductor as a ELQ ($t_{\rm ee2}$) and transmission as a HLQ ($t_{\rm eh2}$). Using the Bogoliubov–de Gennes (BdG) equation[29] and the method developed by McMillan,[31] we can write the wavefunctions in the ferromagnet and superconductor regions as

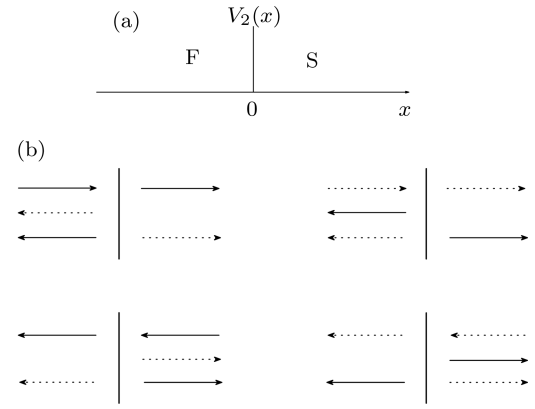


Fig.5. (a) Schematic illustration of an F/I_2/S structure and (b) four types of quasiparticle injection processes in this structure. The solid-line arrow stands for the electron in the ferromagnet or ELQ in the superconductor, while the dotted-line arrow stands for the hole in the ferromagnet or HLQ in the superconductor.

$$\psi_{1\sigma}(x) = \begin{cases} \begin{pmatrix}1\\0\end{pmatrix} \mathrm{e}^{\mathrm{i}k_{\rm e}^{\sigma}x} + r_{\rm eh2}\begin{pmatrix}0\\1\end{pmatrix}\sqrt{\dfrac{k_{\rm e}^{\sigma}}{k_{\rm h}^{\bar\sigma}}}\mathrm{e}^{\mathrm{i}k_{\rm h}^{\bar\sigma}x} + r_{\rm ee2}\begin{pmatrix}1\\0\end{pmatrix}\mathrm{e}^{-\mathrm{i}k_{\rm e}^{\sigma}x}, & \text{for } x \le 0; \\ t_{\rm ee2}\begin{pmatrix}u\\v\end{pmatrix}\sqrt{\dfrac{k_{\rm e}^{\sigma}}{q_{\rm e}^{\rm s}(|u|^2-|v|^2)}}\mathrm{e}^{\mathrm{i}q_{\rm e}^{\rm s}x} + t_{\rm eh2}\begin{pmatrix}v\\u\end{pmatrix}\sqrt{\dfrac{k_{\rm e}^{\sigma}}{q_{\rm h}^{\rm s}(|u|^2-|v|^2)}}\mathrm{e}^{-\mathrm{i}q_{\rm h}^{\rm s}x}, & \text{for } x \ge 0. \end{cases} \tag{A1}$$

Here, $k_{\rm e}^{\sigma} = k_{\rm F}^{\sigma} + mE/(\hbar^2 k_{\rm F}^{\sigma})$, $k_{\rm h}^{\sigma} = k_{\rm F}^{\sigma} - mE/(\hbar^2 k_{\rm F}^{\sigma})$, $k_{\rm F}^{\sigma} = k_{\rm F}\sqrt{1+\eta_\sigma/E_{\rm F}}$ with $\eta_\sigma = 1$ for $\sigma = \uparrow$ and $\eta_\sigma = -1$ for $\sigma = \downarrow$, $q_{\rm e}^{\rm s} = k_{\rm F} + m\Omega/(\hbar^2 k_{\rm F})$, $q_{\rm h}^{\rm s} = k_{\rm F} - m\Omega/(\hbar^2 k_{\rm F})$, $u = \sqrt{(1+\Omega/E)/2}$, and $v = \sqrt{(1-\Omega/E)/2}$ with $\Omega = \sqrt{E^2-\Delta_0^2}$. Coefficients $r_{\rm eh2}$, $r_{\rm ee2}$, $t_{\rm ee2}$ and $t_{\rm eh2}$ correspond to the probability amplitudes for the AR, normal reflection, transmissions within the same branch and those between different branches, respectively. All the coefficients can be determined by matching boundary conditions at $x = 0$:

$$\psi_{1\sigma}(0_-) = \psi_{1\sigma}(0_+),$$

$$\frac{\mathrm{d}\psi_{1\sigma}(x)}{\mathrm{d}x}|_{x=0_-} = \frac{\mathrm{d}\psi_{1\sigma}(x)}{\mathrm{d}x}|_{x=0_+} - 2k_{\rm F}Z_2\psi_{1\sigma}(0). \tag{A2}$$

The wavefunctions for the other three types of quasiparticle injection processes can be obtained in the similar way. We obtain the S-matrix elements in Eq.(1) as

$$r_{\rm ee2} = D_1/D, \tag{A3}$$

$$r_{\rm hh2} = D_2/D, \tag{A4}$$

$$r_{\rm eh2} = -2uv\sqrt{k_{\rm e}^{\sigma}k_{\rm h}^{\bar\sigma}}(q_{\rm h}^{\rm s}+q_{\rm e}^{\rm s})/D, \tag{A5}$$

$$t_{\rm ee2} = -2uk_{\rm e}^{\sigma}(q_{\rm h}^{\rm s}+k_{\rm h}^{\bar\sigma}-2\mathrm{i}k_{\rm F}Z_2)/D, \tag{A6}$$

$$t_{\rm eh2} = 2vk_{\rm e}^{\sigma}(-q_{\rm e}^{\rm s}+k_{\rm h}^{\bar\sigma}-2\mathrm{i}k_{\rm F}Z_2)/D, \tag{A7}$$

where

$$\begin{aligned} D = & -q_{\mathrm{e}}^{\mathrm{s}} q_{\mathrm{h}}^{\mathrm{s}}(u^2-v^2) - (q_{\mathrm{e}}^{\mathrm{s}} u^2 + q_{\mathrm{h}}^{\mathrm{s}} v^2)(k_{\mathrm{h}}^{\bar{\sigma}} - 2\mathrm{i}k_{\mathrm{F}} Z_2) \\ & - (q_{\mathrm{e}}^{\mathrm{s}} v^2 + q_{\mathrm{h}}^{\mathrm{s}} u^2)(k_{\mathrm{e}}^{\sigma} + 2\mathrm{i}k_{\mathrm{F}} Z_2) \\ & - (u^2-v^2)(k_{\mathrm{e}}^{\sigma} + 2\mathrm{i}k_{\mathrm{F}} Z_2)(k_{\mathrm{h}}^{\bar{\sigma}} - 2\mathrm{i}k_{\mathrm{F}} Z_2), \end{aligned} \tag{A8}$$

$$\begin{aligned} D_1 = & q_{\mathrm{e}}^{\mathrm{s}} q_{\mathrm{h}}^{\mathrm{s}}(u^2-v^2) + (q_{\mathrm{e}}^{\mathrm{s}} u^2 + q_{\mathrm{h}}^{\mathrm{s}} v^2)(k_{\mathrm{h}}^{\bar{\sigma}} - 2\mathrm{i}k_{\mathrm{F}} Z_2) \\ & - (q_{\mathrm{e}}^{\mathrm{s}} v^2 + q_{\mathrm{h}}^{\mathrm{s}} u^2)(k_{\mathrm{e}}^{\sigma} - 2\mathrm{i}k_{\mathrm{F}} Z_2) \\ & - (u^2-v^2)(k_{\mathrm{e}}^{\sigma} - 2\mathrm{i}k_{\mathrm{F}} Z_2)(k_{\mathrm{h}}^{\bar{\sigma}} - 2\mathrm{i}k_{\mathrm{F}} Z_2), \end{aligned} \tag{A9}$$

and

$$\begin{aligned} D_2 = & q_{\mathrm{e}}^{\mathrm{s}} q_{\mathrm{h}}^{\mathrm{s}}(u^2-v^2) - (q_{\mathrm{e}}^{\mathrm{s}} u^2 + q_{\mathrm{h}}^{\mathrm{s}} v^2)(k_{\mathrm{h}}^{\bar{\sigma}} + 2\mathrm{i}k_{\mathrm{F}} Z_2) \\ & + (q_{\mathrm{e}}^{\mathrm{s}} v^2 + q_{\mathrm{h}}^{\mathrm{s}} u^2)(k_{\mathrm{e}}^{\sigma} + 2\mathrm{i}k_{\mathrm{F}} Z_2) \\ & - (u^2-v^2)(k_{\mathrm{e}}^{\sigma} + 2\mathrm{i}k_{\mathrm{F}} Z_2)(k_{\mathrm{h}}^{\bar{\sigma}} + 2\mathrm{i}k_{\mathrm{F}} Z_2). \end{aligned} \tag{A10}$$

For the NM/I_1/F junction, due to the absence of the superconductor, all the AR and transmission between the ELQ and HLQ branches disappear. In a similar way, we obtain the S-matrix elements in Eq.(2) as

$$r_{\mathrm{ee1}} = \frac{-2k_{\mathrm{F}} Z_1 + \mathrm{i}(k_{\mathrm{e}}^{\sigma} - q_{\mathrm{e}}^{\mathrm{n}})}{2k_{\mathrm{F}} Z_1 - \mathrm{i}(k_{\mathrm{e}}^{\sigma} + q_{\mathrm{e}}^{\mathrm{n}})}, \tag{A11}$$

$$r'_{\mathrm{ee1}} = \frac{2k_{\mathrm{F}} Z_1 + \mathrm{i}(k_{\mathrm{e}}^{\sigma} - q_{\mathrm{e}}^{\mathrm{n}})}{-2k_{\mathrm{F}} Z_1 + \mathrm{i}(k_{\mathrm{e}}^{\sigma} + q_{\mathrm{e}}^{\mathrm{n}})}, \tag{A12}$$

$$t_{\mathrm{ee1}} = \frac{2\mathrm{i}\sqrt{k_{\mathrm{e}}^{\sigma} q_{\mathrm{e}}^{\mathrm{n}}}}{-2k_{\mathrm{F}} Z_1 + \mathrm{i}(k_{\mathrm{e}}^{\sigma} + q_{\mathrm{e}}^{\mathrm{n}})}, \tag{A13}$$

$$r'_{\mathrm{hh1}} = \frac{-2k_{\mathrm{F}} Z_1 - \mathrm{i}(k_{\mathrm{h}}^{\bar{\sigma}} - q_{\mathrm{h}}^{\mathrm{n}})}{2k_{\mathrm{F}} Z_1 - \mathrm{i}(k_{\mathrm{h}}^{\bar{\sigma}} + q_{\mathrm{h}}^{\mathrm{n}})}, \tag{A14}$$

$$t'_{\mathrm{hh1}} = \frac{2\mathrm{i}\sqrt{k_{\mathrm{h}}^{\bar{\sigma}} q_{\mathrm{h}}^{\mathrm{n}}}}{-2k_{\mathrm{F}} Z_1 + \mathrm{i}(k_{\mathrm{h}}^{\bar{\sigma}} + q_{\mathrm{h}}^{\mathrm{n}})}, \tag{A15}$$

where Z_1 is the dimensionless barrier strength for the NM/I_1/F junction, $q_{\mathrm{e}}^{\mathrm{n}} = k_{\mathrm{F}} + mE/(\hbar^2 k_{\mathrm{F}})$, and $q_{\mathrm{h}}^{\mathrm{n}} = k_{\mathrm{F}} - mE/(\hbar^2 k_{\mathrm{F}})$.

References

[1] Andreev A F 1964 *Sov. Phys. JEPT* **19** 1228
[2] Demler E A, Arnold G B and Beasley R M 1997 *Phys. Rev.* B **55** 15174
[3] Andreev A V, Buzdin A and Osgood III R M 1991 *Phys. Rev.* B **43** 10124
[4] Sun G Y, Xing D Y, Dong J M and Liu M 2002 *Phys. Rev.* B **65** 174508
[5] Fulde P and Ferrell A 1964 *Phys. Rev.* **135** A550
[6] Larkin A and Ovchinnikov Y 1965 *Sov. Phys. JETP* **20** 726
[7] Kontos T, Aprili M, Lesueur J and Grison X 2001 *Phys. Rev. Lett.* **86** 304
[8] Ryazanov V V, Oboznov V A, Rusanov A Y, Veretennikov A V, Golubov A A and Aarts J 2001 *Phys. Rev. Lett.* **86** 2427
[9] Baladie I and Buzdin A 2001 *Phys. Rev.* B **64** 224514
[10] Halterman K and Valls O T 2001 *Phys. Rev.* B **65** 014509
[11] Halterman K and Valls O T 2002 *Phys. Rev.* B **66** 224516
[12] Bergeret F S, Volkov A F and Efetov K B 2002 *Phys. Rev.* B **65** 134505
[13] Zareyan M, Belzig W and Nazarov Y V 2002 *Phys. Rev.* B **65** 184505
[14] Golubov A A, Kupriyanov M Yu and Ll'ichev E 2004 *Rev. Mod. Phys.* **76** 411
[15] Dong Z C, Xing D Y and Dong J M 2001 *Acta Phys. Sin.* **50** 556 (in Chinese)
[16] Dong Z C 2005 *Chin. Phys.* **14** 1209
[17] Yu H L and Dong Z C 2007 *Chin. Phys.* **16** 3072
[18] Zhao K, Feng J F, Huang Y H and Wong H K 2005 *Chin. Phys.* **14** 398
[19] Yu H L, Sun G Y, Yang L Y and Xing D Y 2004 *Physica* C **402** 98
[20] Belzig W, Bruder C and Schön G 1996 *Phys. Rev.* B **54** 9443
[21] Guéron S, Pothier H, Birge N O, Esteve D and Devoret M H 1996 *Phys. Rev. Lett.* **77** 3025
[22] Pannetier B and Courtois H 2000 *J. Low Temp. Phys.* **118** 599
[23] Moussy N, Courtois H and Pannetier B 2001 *Europhys. Lett.* **55** 861
[24] Nikolić B K, Freeicks J K and Miller P 2002 *Phys. Rev. Lett.* **88** 077002
[25] Halterman K and Valls O T 2003 *Physica* C **397** 151
[26] Gupta A K, Crétinon L, Moussy N, Pannetier B and Courtois H 2004 *Phys. Rev.* B **69** 104514
[27] Kontos T, Aprili M, Lesueur J, Grison X and Dumoulin L 2004 *Phys. Rev. Lett.* **93** 137001
[28] Datta S 1995 *Electronic Transport in Mesoscopic Systems* (Cambridge: University Press) Chapters 3 and 6
[29] de Gennes P G 1966 *Superconductivity of Metals and Alloys* (New York: The Benjamin Press)
[30] Blonder G E, Tinkham M and Klapwijk T M 1982 *Phys. Rev.* B **25** 4515
[31] McMillan W L 1968 *Phys. Rev.* **175** 559